AGU PUBLICATIONS

JGR

Journal of Geophysical Research: Biogeosciences

RESEARCH ARTICLE

10.1002/2015JG003027

Key Points:
- Precipitation triggers soil nitrous oxide efflux in wetlands
- Production of soil nitrous oxide highest at wetland edge
- Increase in precipitation events will lead to increase in nitrous oxide efflux

Supporting Information:
- Supporting Information S1

Correspondence to:
I. F. Creed,
icreed@uwo.ca

Citation:
Enanga, E. M., I. F. Creed, N. J. Casson, and F. D. Beall (2016), Summer storms trigger soil N_2O efflux episodes in forested catchments, *J. Geophys. Res. Biogeosci.*, *121*, 95–108, doi:10.1002/2015JG003027.

Received 20 APR 2015
Accepted 3 DEC 2015
Accepted article online 9 DEC 2015
Published online 14 JAN 2016

Summer storms trigger soil N_2O efflux episodes in forested catchments

E. M. Enanga[1], I. F. Creed[1], N. J. Casson[1], and F. D. Beall[2]

[1]Department of Biology, Western University, London, Ontario, Canada, [2]Great Lakes Forestry Centre, Natural Resources Canada, Sault Ste. Marie, Ontario, Canada

Abstract Climate change and climate-driven feedbacks on catchment hydrology and biogeochemistry have the potential to alter the aquatic versus atmospheric fate of nitrogen (N) in forests. This study investigated the hypothesis that during the forest growth season, topography redistributes water and water-soluble precursors (i.e., dissolved organic carbon and nitrate) for the formation of gaseous N species. Soil nitrous oxide (N_2O) and nitrogen (N_2) efflux and soil physical and chemical properties were measured in a temperate forest in Central Ontario, Canada from 2005 to 2010. Hotspots and hot moments of soil N_2O and N_2 efflux were observed in topographic positions that accumulate precipitation, which likely triggered the formation of redox conditions and in turn intercepted the conversion of nitrate N flowing to the stream by transforming it to N_2O and N_2. There was a strong relationship between precipitation and N_2O efflux ($y = 0.44x^{1.22}$, $r^2 = 0.618$, $p < 0.001$ in the inner wetland; $y = 1.30x^{1.16}$ $r^2 = 0.72$, $p < 0.001$ in the outer wetland) and significantly different N_2:N_2O ratios in different areas of the wetland (19.6 in the inner wetland and 10.1 in the outer wetland). Soil $N_2O + N_2$ efflux in response to precipitation events accounted for 16.1% of the annual N input. A consequence of the higher frequency of extreme precipitation events predicted under climate change scenarios is the shift from an aquatic to atmospheric fate for N, resulting in a significant forest N efflux. This in turn creates feedbacks for even warmer conditions due to increased effluxes of potent greenhouse gases.

1. Introduction

More than one half of Canada's non-Arctic land base [*Canada's National Forest Inventory's*, 2013] and about one third of the U.S. [*Smith et al.*, 2009] is forested. Despite recent decreases in anthropogenic N emissions [e.g., *Kothawala et al.*, 2011; *International Joint Commission*, 2012; *Eshleman et al.*, 2013], elevated N levels continue to affect temperate forests [*Sirois et al.*, 2001; *Lovett and Goodale*, 2011]. Atmospherically deposited N in forests can be stored in the soil, transformed by organisms, exported in dissolved forms to surface waters, or exported as nitrous oxide (N_2O) and dinitrogen (N_2) gas to the atmosphere through denitrification [*Pardo et al.*, 2011]. Forest soils may contribute substantial amounts of N_2O [*Ambus and Roberston*, 2006]. A predictive understanding of the fate of atmospherically deposited N is important because exports to aquatic and atmospheric systems can have negative effects on society—e.g., global warming, ozone depletion resulting in UV depletion, and degraded drinking water quality. However, scientific understanding of N cycling has not kept pace with other biogeochemical processes due to spatial and temporal heterogeneity [*McClain et al.*, 2003] and the methodological challenges of measuring and estimating N_2O fluxes [*Groffman et al.*, 2006].

Recent observations suggest that the frequency of intense and heavy precipitation events has increased in many areas of North America and Europe [*Intergovernmental Panel on Climate Change*, 2013]. Precipitation influences soil water availability that in turn regulates soil N cycling rates and pathways on landscapes [*Lohse et al.*, 2009]. Precipitation-induced saturation of soils results in low O_2 concentrations, causing low redox potentials that favor N_2O production, and prolonged saturation can lead to further reduction of N_2O to N_2 [*Gambrell and Patrick*, 1978] (Figure 1). Several studies have reported increased N_2O production with increased precipitation using modeling techniques [*Li et al.*, 1992], laboratory experiments [*Rubol et al.*, 2012; *Hall et al.*, 2014], and field experiments [*Vilain et al.*, 2010]. Precipitation that reaches the forest floor is redistributed due to topography [*Zhu et al.*, 2014], and so topography plays an important role in regulating not only soil nutrient pools but also soil temperature, moisture, and redox, thereby influencing microbial biomass and N cycling processes [*Ambus*, 1998; *Hazlett and Foster*, 2002; *Gu et al.*, 2011;

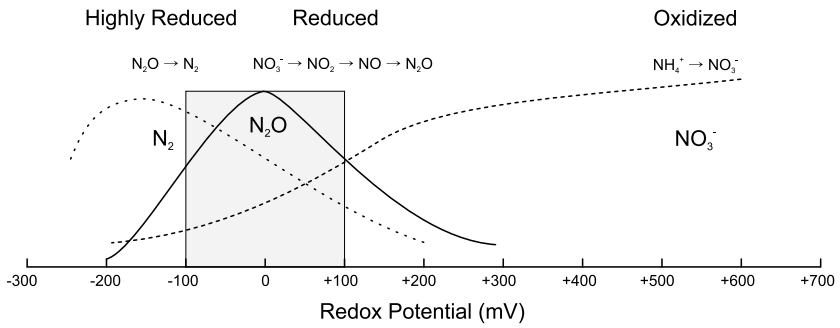

Figure 1. Conceptual figure showing the relationship between reduction-oxidation (redox) potential conditions and the end products of denitrification (modified from *Kralova et al.* [1992]).

Stewart et al., 2014]. A predictive understanding of the links between precipitation, topography, and soil properties that regulate soil N cycling processes may lead to improved estimates of soil N_2O efflux from natural landscapes [*Creed et al.*, 2013; *Duncan et al.*, 2013; *Anderson et al.*, 2015].

The purpose of this study is to explore topographic controls on temporal and spatial patterns of redox potential and their relation to N_2O and subsequent N_2 production along a hillslope during the growing season in a temperate forest. It was hypothesized that during the snow-free season, topography redistributes water and water-soluble precursors of the formation of gaseous N species (dissolved organic carbon (DOC) and nitrate (NO_3^-)), creating hotspots of soil N_2O efflux in topographic features that become hot moments in response to storms. To test the hypothesis, the following questions were asked: Q1: How does soil N_2O and N_2 efflux vary with topographic feature (uplands, lowlands, wetlands)? Q2: How do variations in the soil physical (temperature, moisture, redox potential) or chemical (DOC and NO_3^-) properties within topographic features relate to soil N_2O efflux? Q3: Do episodic variations in the soil physical or chemical properties caused by summer storms correlate with changes in the rates of soil N_2O efflux? The hypothesis and associated questions were tested in the forested landscape of the Great Lakes-St. Lawrence forest region at the northern edge of the temperate forest biome of North America.

2. Materials and Methods

2.1. Study Area

The Turkey Lakes Watershed (47°03′00″N and 84°25′00″W) is a 10.5 km^2 long-term experimental watershed located at the northern edge of the Great Lakes-St. Lawrence forest region near the eastern shore of Lake Superior in the Algoma Highlands of Central Ontario, 60 km north of Sault Ste. Marie (Figure 2) [*Jeffries et al.*, 1988]. The watershed is characterized by a continental climate, with a mean total annual precipitation of 1189 mm and mean annual temperature of 4.6°C based on a 30-year (1981–2010) data record from the meteorological recording station located just outside the watershed. Total annual precipitation and stream discharge have generally decreased over this 30 year time span [*Mengistu et al.*, 2014] in response to a gradual increasing trend in mean annual temperature (Figure 3). The watershed rests on Precambrian silicate greenstone formed from metamorphosed basalt. Topographic relief is about 400 m, ranging from 644 m at the apex of Batchawana Mountain to 244 m at the outlet of the Batchawana River that drains into Lake Superior. A thin discontinuous glacial till of varying depth overlays the bedrock, ranging from < 1 m in high elevation areas to 1–2 m in lower elevation areas and occasionally as much as 65 m in bedrock depressions. The podzolic soils in the tills are generally thin and undifferentiated near ridges, which gradually thicken, differentiate, and increase in organic content on topographic benches and toward the stream, and there are highly humified organic deposits in wetlands [*Canada Soil Survey Committee*, 1978]. The watershed is covered by an uneven-aged forest, including mature to overmature trees and some areas of old growth, which is dominated by 90% sugar maple (*Acer saccharum* Marsh.), dotted with patches of white pine (*Pinus strobus* L.), yellow birch (*Betula alleghaniensis* Britton), ironwood (*Ostrya virginiana* (Mill.) K. Koch), white spruce (*Picea glauca* Moench Voss.), and red oak (*Quercus rubra* L.) in upland areas [*Wickware and Cowell*, 1985]. This study is a companion to one that focused on topographic effects on soil carbon dioxide efflux from the same watershed [*Webster et al.*, 2008a, 2008b].

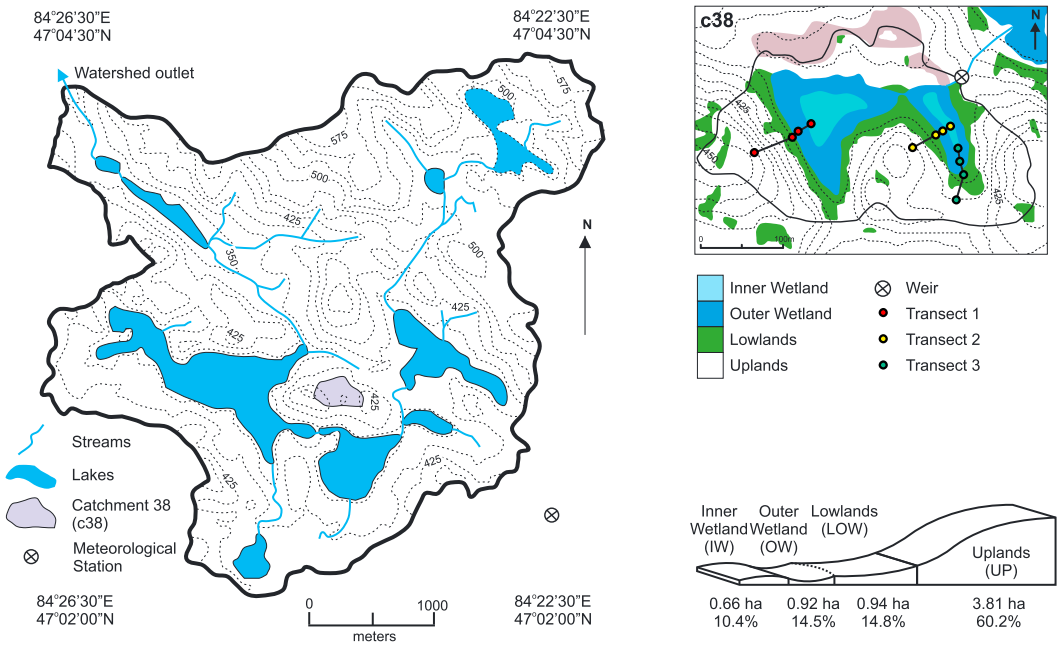

Figure 2. Map of the Turkey Lakes Watershed near Sault Ste. Marie, Ontario, Canada.

2.2. Experimental Design

Within the Turkey Lakes Watershed, catchment 38 (c38) occupies an area of 6.33 ha and includes a major wetland (25% of catchment area) (Figure 2). Three replicate transects were established, and each was instrumented to monitor environmental conditions and collect gas samples from sampling sites at four topographic positions, including the inner wetland (IW), outer wetland (OW), lowlands (LOW), and uplands (UP). Each sampling site was instrumented for continuous monitoring of soil temperature, moisture and redox potential, synoptic monitoring of soil solution for DOC and dissolved NO_3^-, and synoptic sampling of soil N_2O efflux. Synoptic samples were collected from postsnowmelt in early June to presnowfall in late September and were targeted to coincide with precipitation events, with baseline samples collected during days without precipitation.

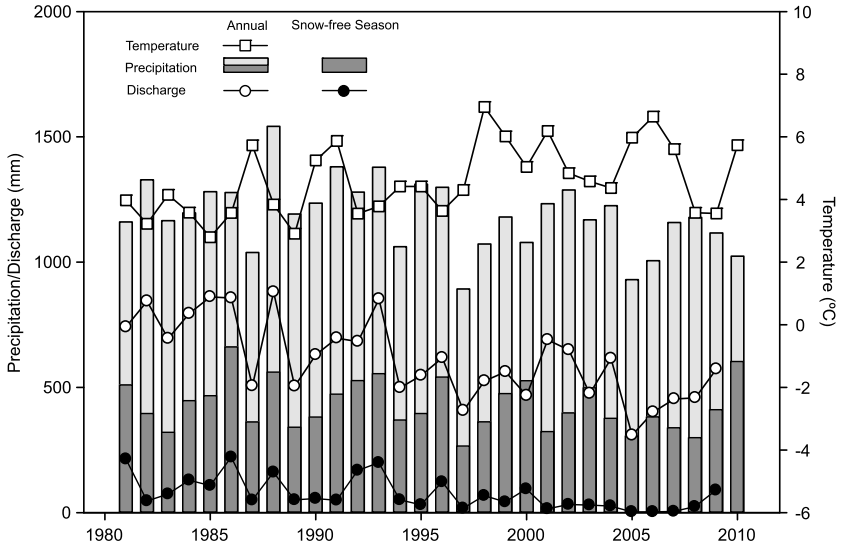

Figure 3. Annual precipitation, discharge, and temperature and snow-free season (June to September) precipitation and discharge in the Turkey Lakes Watershed from 1981 to 2010.

2.3. Data Collection

2.3.1. Defining Topographic Features

The IW (raised centre of the wetland), OW (depressed ring around the edge of the wetland), LOW (flat to gently sloped area at the base of the hillslope), and UP (steep area at the middle of the hillslope) were defined using a lidar-derived 5 m digital elevation model of the c38 catchment. Five terrain derivatives were selected to represent topographic characteristics: percent height relative to local pits and peaks, percent height relative to local channels and divides, wetness index, slope curvature, and slope gradient. These terrain derivatives were used to classify LOW and UP topographic positions using a fuzzy membership function defined based on extensive field experience of scientists working in the watershed. The wetland area was delineated using a probabilistic approach to determine the likelihood of an area being flat or in a depression as described in *Lindsay and Creed* [2006]. The boundary of the IW was determined from a ground-based survey of the wetland on a 5 m grid. The field survey was then spatially interpolated, and the IW was defined as the portion of the wetland with peat depths greater than 70 cm. The OW was defined as the area outside the IW but within the delineated wetland. See *Webster et al.* [2011] for additional details of how topographic features were defined.

2.3.2. Catchment Hydrology

Meteorological data including daily total precipitation and daily average air temperature were obtained from the Canadian Air and Precipitation Monitoring Network (CAPMoN) station operated by Environment Canada and located just outside the Turkey Lakes Watershed (47°02′06″N and 84°22′52″W). Daily discharge was derived from continuously measured stream stage at V notch weirs. Wetland water table depth was continuously measured using a water level logger (WT-HR Water Height Data Logger, TruTrack Inc., Christchurch, NZ) at the IW position from 2005 to 2010, with positive values indicating water above the ground surface.

2.3.3. Soil Physical and Chemical Properties

Soil temperature (2006–2010), soil moisture (2005–2010), and soil redox potential (2005) were measured at each sampling site [*Webster et al.*, 2008a]. Redox potential was determined by measuring the voltage between a platinum electrode and a potassium chloride reference electrode. All the instruments were wired to data loggers (Campbell Scientific CR10X) using multiplexors, which were powered by batteries charged by solar panels. All environmental data were collected every 5 min and averaged every 30 min by the data logger. Soil pore water samples were collected within 48 h of N_2O sampling using suction lysimeters (Model 1900, Soil Moisture Corp., Santa Barbara, CA) installed at each sampling site up to a depth of 10 cm into the mineral soil or peat [*Webster et al.*, 2008a]. The samples were then filtered through 0.45 μm polysulfone membrane filters (Supor 450, Pall Gelman Science, Michigan, USA) and then analyzed for DOC using oxidative combustion coupled with infrared detection (Shimadzu TOC-V, Tokyo, Japan) and for NO_3^- using flow injection colorimetry (Lachat QuikChem 8000, Milwaukee, WI).

2.3.4. Soil N_2O and N_2 Efflux

Ground-based static chambers [*Hutchinson and Livingston*, 2001] were used to monitor soil N_2O efflux at each sampling site from 2006 to 2010. Square collars measuring 45.7 × 45.7 cm (2088 cm^2) were inserted 10–20 cm into the soil. Samples were collected between 1000 h and 1400 h. Collars were placed at sampling sites for each of the IW, OW, LOW, and UP positions on each of the three transects. Vented polyvinylchloride chambers (14.6 L) were placed over the collars for an hour to inhibit the air turbulence during chamber placement and to minimize pressure changes during sampling that would affect accumulation of N_2O during sampling.

Nitrous oxide samples were collected at time 0, 20, 40, and 60 min from each of the collars using a 30 mL syringe fitted with a needle. Prior to sample collection, the sampling tube was flushed five times with 30 mL of air from the chamber to clear tubing of previous sample and ensure mixing of the air inside the chamber. Nitrous oxide samples equivalent to 30 mL of chamber air were then drawn into a sampling syringe—5 mL of the sample was flushed through the sampling needle to rinse it of any residual atmospheric air. The remaining 25 mL of the sample was injected into sealed 12.1 mL pre-evacuated Exetainers® that contained a small amount of magnesium perchlorate as a desiccant, which was transported to the laboratory for analysis. Nitrous oxide concentration was determined using gas chromatography on an SRI 8610C (SRI Inc., Las Vegas, NV) equipped with an electron capture detector.

Nitrous oxide fluxes were determined by calculating the linear regression of the slope of N_2O concentration within the chambers with time. The N_2O fluxes were scaled up to the total headspace volume derived from the addition of chamber volume and the collar volume above the soil surface and cross-sectional area of the

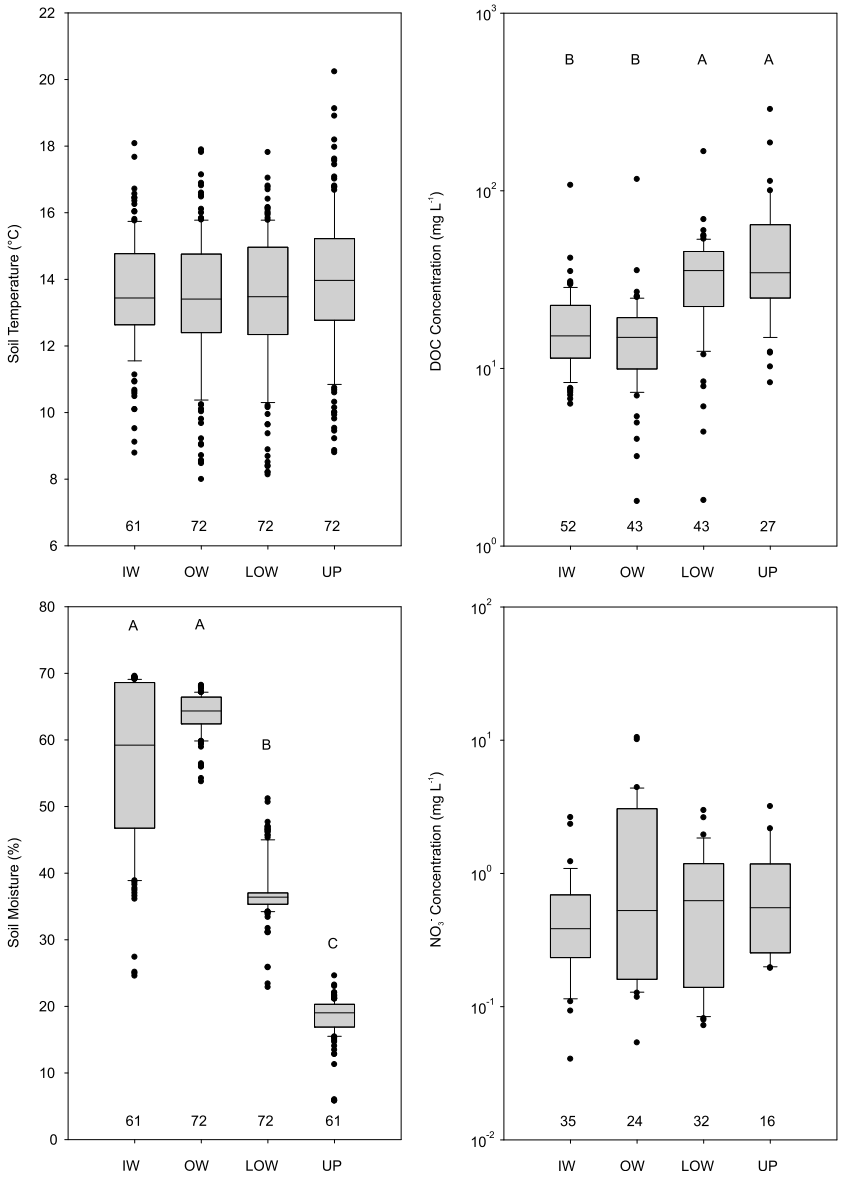

Figure 4. Soil temperature, moisture, dissolved organic carbon (DOC), and nitrate (NO_3^-) from 2006 to 2010 in the inner wetland (IW), outer wetland (OW), lowlands (LOW), and uplands (UP) topographic positions averaged across three transects. Different letters indicate significant differences among soil characteristics by topographic position based on ANOVAs on ranks with post hoc Dunn's tests ($p < 0.05$). Numbers indicate the sample sizes (one value per day).

collar and corrected for ambient pressure and temperature. Only positive soil N_2O efflux measurements were included in the analysis. There were a few negative N_2O fluxes (200 of 1263, 16%) that were small in magnitude (-0.01 to $-92.10\,g\,N\,ha^{-1}\,d^{-1}$); while only positive N_2O measurements were included in the analysis, inclusion of both positive and negative measurements did not change the final results (data not shown).

Dinitrogen fluxes were estimated using the acetylene inhibition technique [*Tiedje et al.*, 1989] in the topographic positions where N_2 production would be likely (i.e., IW and OW) based on low redox conditions and low oxygen levels [*Morse et al.*, 2015]. Twenty-five square metal collars (45.7×45.7 cm) were installed: five controls and 10 treatments in each of the IW and OW positions. The collars were left to settle for a year before gas samples were collected in July 2010. Soil moisture content within each collar was manipulated with simulated precipitation equivalent to 10 mm using deionized water prior to acetylene treatment. The five control collars had no acetylene added, and samples were collected at 15 min intervals for one hour similar to the treated collars. The 20 treatment collars were subjected to a 30% acetylene volume relative to

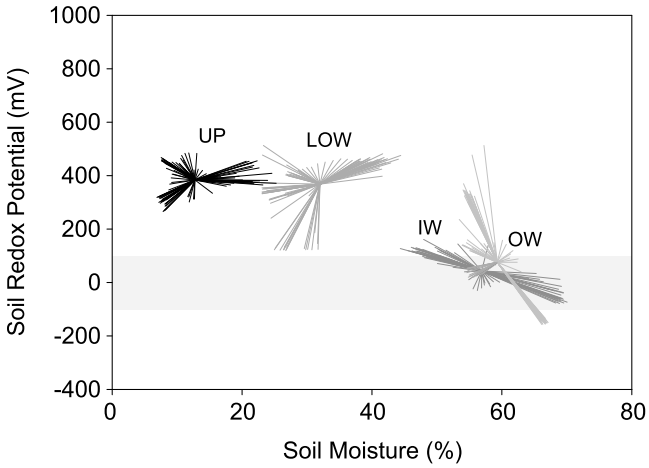

Figure 5. Relationship between redox potential and soil moisture conditions. The centroids show the mean redox potential and soil moisture for each topographic position, with the ends of the branches showing each observed value. The shaded area represents the range of redox potentials appropriate for N_2O production.

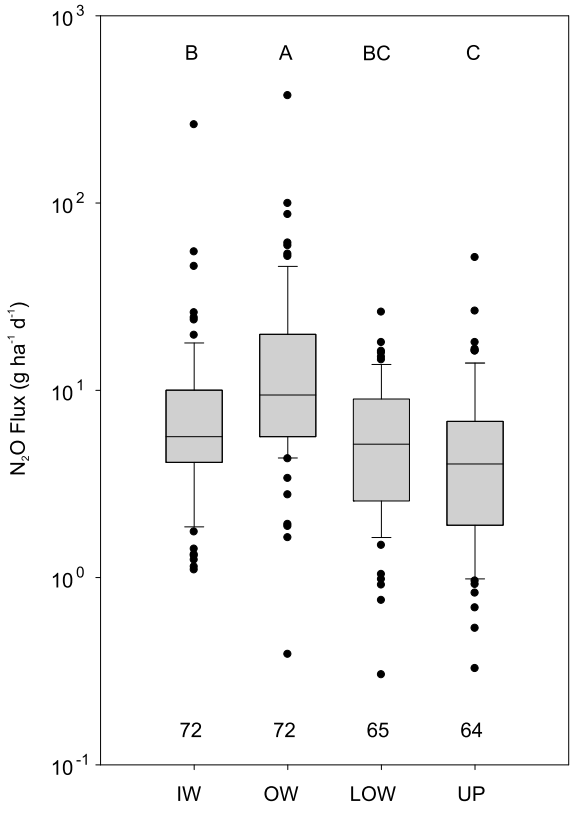

Figure 6. Soil N_2O efflux from 2006 to 2010 in the inner wetland (IW), outer wetland (OW), lowlands (LOW), and uplands (UP) topographic positions averaged across three transects. Different letters indicate significant differences among soil N_2O efflux by topographic position based on ANOVAs on ranks with post hoc Dunn's tests ($p < 0.05$). Numbers indicate the sample sizes (one value per day).

headspace volume. The 30% acetylene was selected from a 10% incremental range from 0 to 50 % based on a field-based optimization experiment that showed the most rapid increase in N_2O to reach a maximum within 1 h (data not shown). Acetylene gas was allowed to percolate into the soil for one hour, after which the chambers were lifted off the collars and aired out. The chamber was replaced on the collar, sealed by adding water to the grooves on the collars, and gas samples were collected immediately after placing the chamber onto the collar and at 15 min intervals for 1 h. Dinitrogen was estimated as the difference in N_2O produced from the acetylene treated and untreated (control) collars, and the N_2:N_2O ratio was calculated.

Atmospheric N deposition measurements have been collected at the CAPMoN since 1981. Wet deposition measurements were collected using a wet-only precipitation chemistry sampler, and samples for daily air chemistry measurements were collected using filter packs. Dry deposition values were calculated using daily deposition velocities [*Sirois and Vet*, 1988]. The CAPMoN air concentration measurements included nitrate (NO_3^-) and ammonium (NH_4^+). Nitrate, nitric acid (HNO_3), and NH_4^+ measurements were determined from precipitation and dry air [*Sirois and Vet*, 1988]. Total organic N was estimated as 15% of total N, based on average regional deposition of total organic N [*Dillon et al.*, 1991].

To calculate the total annual $N_2O + N_2$ efflux caused by precipitation, the relationship between precipitation and N_2O efflux was used to estimate N_2O efflux for all days where precipitation exceeded 3 mm and the water table depth was less than 10 mm from 2005 to 2010 in all topographic positions where there was a significant relationship and the N_2:N_2O ratios were used to estimate N_2 efflux. The daily fluxes were multiplied by the area of each position and then summed to give a

Table 1. Spearman Rank Correlations Between Soil N_2O Efflux and Soil Physical and Chemical Properties in the Inner Wetland (IW), Outer Wetland (OW), Lowlands (LOW), and Uplands (UP) Topographic Positions[a]

	IW		OW		LOW		UP	
Control Variable	*r*	*p*	*r*	*p*	*r*	*p*	*r*	*P*
Water table depth (mm)	0.111	0.353	**−0.308**	**0.009**	**0.372**	**0.002**	**0.425**	**0.001**
Soil temperature (°C)	−0.115	0.374	−0.039	0.745	**0.355**	**0.004**	0.065	0.612
Moisture (%)	0.098	0.453	**−0.288**	**0.014**	**0.264**	**0.034**	**0.342**	**0.006**
Soil pore water NO_3^-	**0.443**	**0.021**	0.404	0.055	−0.103	0.653	0.000	0.989
Soil pore water DOC	−0.091	0.479	0.182	0.196	0.031	0.840	0.156	0.360

[a]Bolded values indicate significant relationships ($p<0.05$).

total $N_2O + N_2$ gaseous export in response to precipitation during the forest growth season for each year. The proportion of N deposition that was N efflux was then calculated and averaged from 2005 to 2010.

2.4. Data Analyses

Daily soil temperature, moisture, and DOC, NO_3^-, and N_2O efflux measurements from the three transects were averaged to give one value per day per topographic position and then compared using analyses of variance (ANOVAs) on ranks with post hoc Dunn's tests ($p < 0.05$). The relationships between soil N_2O efflux and water table depth, soil temperature, soil moisture, DOC, and NO_3^- were investigated using Spearman rank correlations.

The relationship between precipitation and N_2O efflux was assessed using nonlinear regression with a power function for all four topographic positions. To determine the effect of storm events on soil N_2O efflux, the relationship between precipitation and N_2O efflux was investigated by defining effective precipitation as the amount of precipitation that fell on the same day that the soil N_2O efflux was measured and on the preceding day (to capture overnight precipitation). Days when precipitation exceeded the forest canopy interception capacity (≥3 mm) and when the water table depth was < 10 mm above the ground surface were used to isolate the effects of the effective precipitation event and ensure there was not excessive standing water in the wetland. An analysis of covariance (ANCOVA) was performed to determine if the effective precipitation versus N_2O relationship varied among topographic positions. Monte Carlo simulation was employed to estimate the potential distribution of N_2 efflux using the observed soil N_2O efflux values and N_2:N_2O ratios determined using acetylene inhibition experiments. Statistical analyses were performed in SigmaPlot v. 12, SPSS v. 22, and Microsoft Excel.

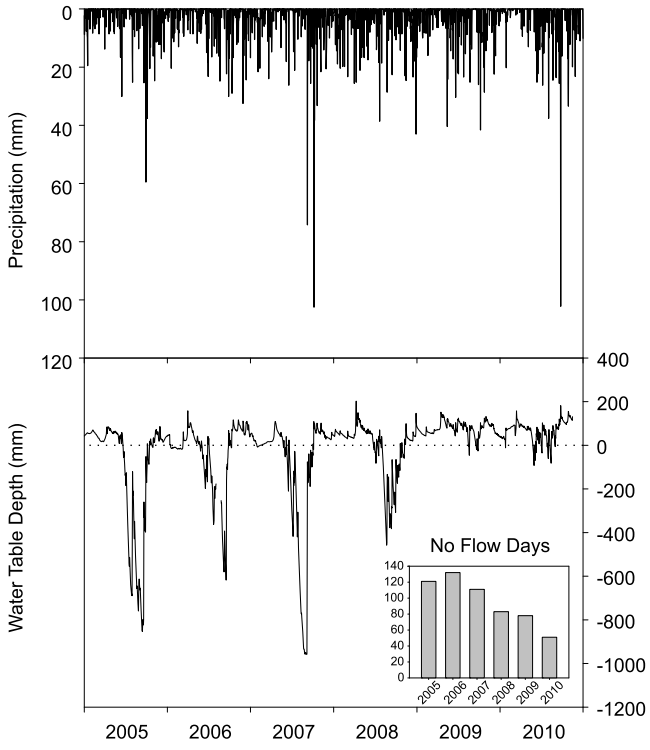

Figure 7. Precipitation and water table depth in c38 from 2005 to 2010 with number of days with no flow inset.

3. Results

3.1. Catchment Hydrology

There was a declining trend in precipitation and discharge in the Turkey Lakes Watershed since 1981 (Figure 3). However, among the years investigated in this study (2005–2010), precipitation and discharge were lowest in 2005 and tended to increase from 2006 to 2010 (Figure 3).

3.2. Soil Physical and Chemical Properties

Soil temperature was consistent across topographic positions, but there was significant variation in soil moisture, with

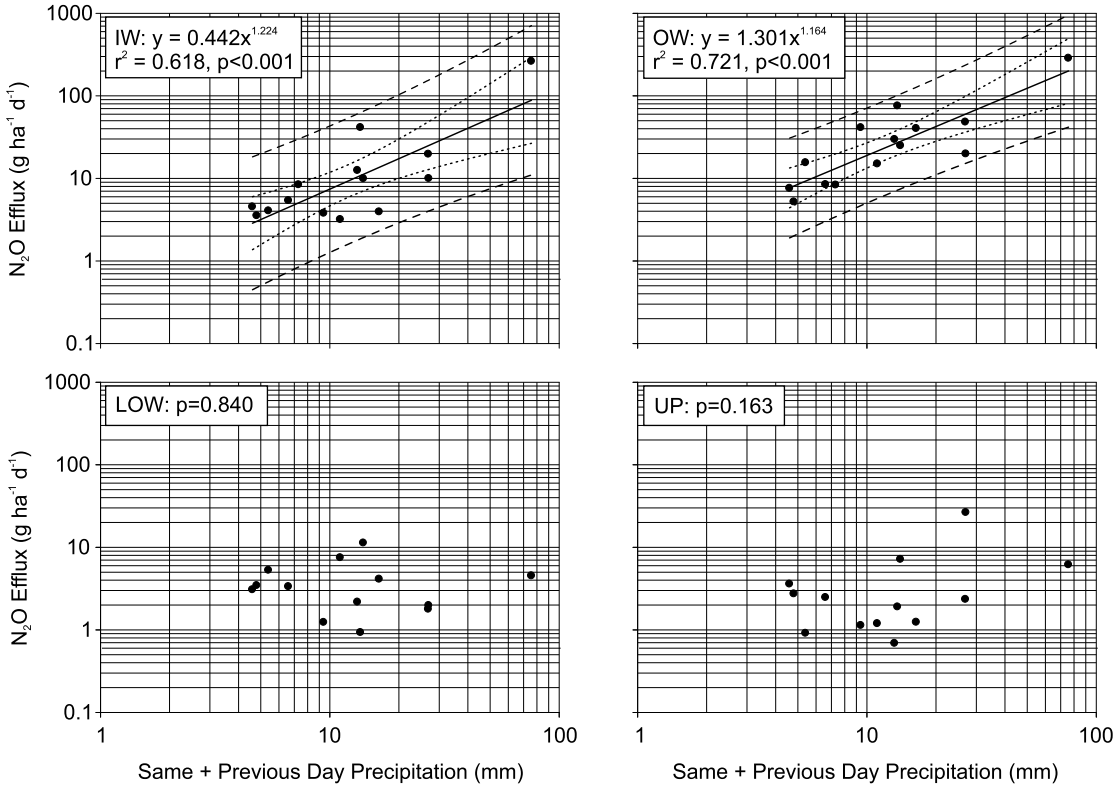

Figure 8. Relationship between effective precipitation (same day plus previous day) and soil N_2O efflux on a subset of days where same day plus previous day precipitation exceeded 3 mm and the water table depth was less than 10 mm with the 95% confidence intervals (dotted lines) and 95% prediction intervals (dashed lines).

the IW and OW having significantly higher moisture than the LOW and UP (Figure 4). Unfortunately, redox potential data were only available for 2005. In the year when redox was measured, appropriate redox conditions for N_2O production, namely, between −100 and +100 mV [*Kralova et al.*, 1992]), were only found at the IW and OW positions and only occurred when soil moisture ranged from 50 to 70% (Figure 5). In all of the years of measurement, the soil moisture regimes at the UP position never reached the 50 to 70% volumetric water content range, and therefore, it is unlikely that redox conditions necessary to support sustained N_2O existed at the UP positions. There was significantly more DOC in the LOW and UP positions compared to the IW and OW positions, and there was little difference in NO_3^- among the topographic positions (Figure 4).

3.3. Soil N_2O and N_2 Efflux

There were significant differences in soil N_2O efflux among the topographic positions; the OW position had higher soil N_2O efflux than all other topographic positions (Figure 6). While significant relationships existed between soil properties and soil N_2O efflux, these relationships were generally quite weak ($|r|$ ranged from 0.25 to 0.44) (Table 1). Soil moisture patterns from 2006 to 2010 (Figure 4) closely approximated those of the soil N_2O efflux patterns (Figure 6), while DOC and NO_3^- patterns (Figure 4) did not show a direct association with N_2O. Although the soil moisture and soil N_2O efflux patterns were similar, there was less variation in soil moisture (coefficients of dispersion of 0.24 in IW, 0.04 in OW, 0.14 in LOW, and 0.18 in UP) than in soil N_2O efflux (coefficients of dispersion of 1.08 in IW, 1.45 in OW, 1.33 in LOW, and 1.09 in UP). To investigate what other factor could be influencing soil N_2O efflux, the relationship between effective precipitation (which influences moisture) and soil N_2O efflux was investigated.

Precipitation varied considerably from 2005 to 2010; years with less precipitation resulted in lower water tables and more no flow days (Figure 7). Looking at the effect of precipitation on soil N_2O efflux, there was no significant relationship between N_2O efflux and precipitation when all data were included (data not shown). To investigate the effect of storm events on N_2O efflux, days with effective precipitation events (same day plus previous) greater than 3 mm and days where water table depth was less than 10 mm were

Table 2. Ratios of N_2 to N_2O in the Inner Wetland (IW) and Outer Wetland (OW) Topographic Positions Determined Using a Field Acetylene Inhibition Experiment

	Average	Standard Deviation	Minimum	Maximum
IW ($n = 10$)	19.585	9.659	6.831	33.616
OW ($n = 10$)	10.056	6.265	3.986	21.785

investigated. We chose the 10 mm threshold to include all possible data when soils were not inundated. We found that when data greater than 10 mm were included, relationships that were significant were no longer significant. In the LOW and UP positions, there were no significant relationships between the magnitude of effective precipitation and the soil N_2O efflux from the LOW and UP positions (Figure 8). In contrast, there were significant relationships between effective precipitation and soil N_2O efflux in the IW and OW topographic positions (Figure 8). The magnitude of effective precipitation explained 62% of the variation in soil N_2O efflux from the IW position ($y = 0.442x^{1.224}$, $r^2 = 0.618$, $p < 0.001$) and 72% of the variation in the OW position ($y = 1.301x^{1.164}$, $r^2 = 0.721$, $p < 0.001$). There was one 48 h period with a large storm (75 mm) and a water table depth less than 10 mm. This data point also had the largest N_2O efflux in the IW and OW positions. The relationship between effective precipitation and soil N_2O efflux still held when these points were removed (IW: $1.33x^{0.721}$, $p = 0.049$, $r^2 = 0.309$; OW: $1.864x^{0.999}$, $p = 0.005$, $r^2 = 0.523$). An ANCOVA of the relationships between the magnitude of effective precipitation and soil N_2O efflux showed that there were significant differences between the IW and OW topographic positions (d.f. = 1, $F = 22.16$, $p < 0.001$) and no significant interaction. Same day plus previous day precipitation was used to investigate the relationship between N_2O efflux and precipitation, but there were some days where the majority of the precipitation fell the day before sampling. Removing these days from the investigation improved the variation explained in the IW and OW (to 77% and 83%, respectively) but left only six data points.

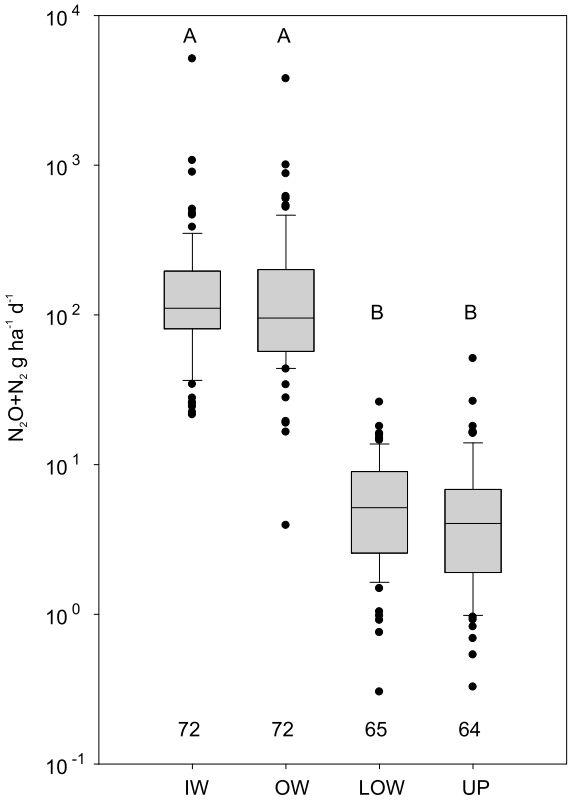

Figure 9. Soil $N_2O + N_2$ efflux from 2006 to 2010 in the inner wetland (IW), outer wetland (OW), lowlands (LOW), and uplands (UP) topographic positions averaged across three transects. In the LOW and UP positions, N_2 was not measured and was assumed to be negligible due to oxic conditions. Different letters indicate significant differences among soil $N_2O + N_2$ efflux by topographic position based on ANOVAs on ranks with post hoc Dunn's tests ($p < 0.05$). Numbers indicate the sample sizes (one value per day).

The average N_2:N_2O ratio in the IW (19.6:1) was significantly higher than the N_2:N_2O ratio in the OW (10.1:1) (Table 2). Using these ratios, the combined $N_2O + N_2$ efflux was higher in the IW and OW positions compared to the LOW and UP positions (Figure 9). Based on these ratios, the effective precipitation versus soil $N_2O + N_2$ efflux was $y = 8.669x^{1.224}$ for the IW and $y = 13.136x^{1.164}$ for the OW. The observed N_2:N_2O ratios were highly variable (IW standard deviation = 9.7 and OW standard deviation = 6.3). Using these ratios in Monte Carlo simulations resulted in highly variable soil N_2 efflux data (Table 3).

The average total $N_2O + N_2$ efflux from the catchment caused by effective precipitation events during the snow-free season, calculated using estimated $N_2O + N_2$ per hectare based on the relationship between effective precipitation and N_2O efflux in the IW and OW positions and the N_2:N_2O ratios, multiplied by the area of each topographic position and summed for all days with effective precipitation events, was 10.0 kg yr^{-1}. This represents 16.1 % of the average annual N input (which was 9.9 kg N ha^{-1} yr^{-1} or 62.7 kg N yr^{-1} for the entire 6.33 ha catchment).

Table 3. Estimates of N_2 Efflux (g ha^{-1} d^{-1}) in the Inner Wetland (IW) and Outer Wetland (OW) Based on Monte Carlo Simulation (10,000 Replicates) Using N_2O Fluxes ($n = 72$ for IW, $n = 72$ for OW) and N_2:N_2O ratios ($n = 10$ for IW, $n = 10$ for OW)

Percentile	IW	OW
2.5th	11.64	7.30
5th	13.58	10.24
25th	35.30	34.53
50th	55.51	60.30
75th	99.48	121.57
95th	152.96	432.03
97.5th	165.46	727.68

4. Discussion

Nitrogen budgets in forested catchments are frequently unbalanced, with inputs exceeding outputs, and the sinks for this excess N are the subject of much debate. Underestimation of gaseous N losses from forest soils is a common hypothesis for this missing sink [*Yanai et al*., 2013], but estimating N_2O and N_2 losses at catchment scales is difficult. Recent studies have had success relating topographic wetness indices to N_2O and N_2 efflux [*Duncan et al*., 2013; *Kulkarni et al*., 2014; *Anderson et al*., 2015], but substantial uncertainty remains. In the present study, 16.1 % of the annual N input was exported as N_2O and N_2 gas from the wetland in response to effective precipitation events. This finding is similar to the few other studies that have included estimates of denitrification in forested watershed N budgets, for instance, *Duncan et al.* [2013] found that denitrification accounted for 16 to 27% of N inputs from an oak forest in Maryland, whereas *Kulkarni et al.* [2014] found that up to half of N inputs to hardwood forests in New Hampshire were lost to denitrification. These results reaffirm the primary role of topography in determining gaseous N fluxes, not only through the distribution of soil moisture and thus appropriate redox conditions but also by delivering the water-soluble reactants necessary for the denitrification reaction.

The UP and LOW positions recorded higher redox potential values (>300 mV) compared to the wetland areas; hence, denitrification was not favored at these positions because the soils were better aerated [*Kralova et al*., 1992; *Foster et al*., 2005; *Morse et al*., 2015].

The OW position experienced a large range of redox potentials, oscillating between oxic (>400 mV) and anoxic (<400 mV). There were dry spells (redox >400 mV) during which nitrification could occur [*Hazlett and Foster*, 2002; *Foster et al*., 2005; *Snider et al*., 2009], replenishing the NO_3^- that was depleted during denitrification from the wet periods (redox <400 mV). Precipitation events that exceeded the forest canopy interception capacity increased the soil moisture content in surface soils with a corresponding decrease in redox potential while at the same time likely bringing more DOC and NO_3^- through the vertical and lateral flow of water, thereby creating conditions that favor N_2O production. The relationship between the magnitude of an effective precipitation event and the amount of soil N_2O flux was more significant in the OW compared to the IW, probably due to the in situ production of precursors of denitrification (DOC and NO_3^-) when redox was high and from the ex situ production of precursors from upland areas that are transported to the OW during these periods of hydrological connectivity [*Cirmo and McDonnell*, 1997; *Lohse et al*., 2009].

The IW position experienced a narrower range of redox potentials. This may have resulted in greater depletion of NO_3^- with minimal to no in situ replenishment because redox conditions were not in the range to promote nitrification and replenish the precursors. In addition, the location of the IW relative to the OW position along the hillslope continuum (the IW is surrounded by the OW) ensured that the IW's main source of inputs through lateral flow is from the OW position. The OW position may be rich in N_2O due to its rapid processing of NO_3^-, which would leave the IW to receive inputs depleted in NO_3^- and rich in N_2O from the OW position and lead to an increase in the denitrification processes that further reduce N_2O to N_2 [*Gambrell and Patrick*, 1978; *Wrage et al*., 2001]. Further reduction of N_2O to N_2 in the absence of adequate NO_3^- would be favored [*Wrage et al*., 2001], potentially explaining the lower N_2O fluxes observed from the IW position relative to the OW position. The observed N_2:N_2O ratio was higher in the IW compared to the OW positions. This suggests that water arriving to the IW is depleted in NO_3^- after passing through the adjacent OW, and therefore, more N_2O is being used as an electron acceptor and reduced to N_2 in the absence of the preferred O_2 or NO_3^- in the IW [*Gambrell and Patrick*, 1978]. Our estimates of N_2:N_2O ratios were quite variable (Table 2), although well within the wide ranges reported in the literature (Table 4). More accurate N_2 estimates are necessary to develop a better predictive understanding N cycling in catchments.

Table 4. Different Methods and Techniques That Have Been Used to Estimate N_2:N_2O Ratios and the Varied Results That Have Been Obtained Over the Years

N_2:N_2O Ratio	Methods	Substrate	Controlling Variables	Reference
0.81 to 200	^{13}N-labeled gases measured from intact cores	Litter from pine and beech forests	Land use	*Speir et al.* [1999]
5.4 to 48	^{15}N applied to hand mixed soil	Tropical forest 10 cm soils	NO_3^- and moisture	*Yang et al.* [2014]
0.01 to 500	^{15}N-labeled N_2 and N_2O collected from mesocosms	Riparian and wetland soils	pH and NO_3^- concentration	*Addy et al.* [1999]
0.5 to 17	^{15}N-labeled N_2 and direct N_2O measured from intact cores	Agricultural soil	C and NO_3^- availability, water filled pore space, and soil texture	*Del Grosso et al.* [2000]
0.3	Acetylene block	Agricultural soil upper 15 cm	NO_3^-	*Blanco-Jarvio et al.* [2011]
3.5 to 9	Acetylene block applied to intact cores	Soil from riparian zone of bottomland hardwood forest	Soil water	*Ullah et al.* [2005]
0.2 to 2	Acetylene block applied to intact cores	Pasture soil	NO_3^- and pH	*Zaman and Nguyen* [2010]
0.24 to 71	Acetylene block applied to intact cores	Agriculture soil	Moisture and NO_3^-	*Menendez et al.* [2008]
0.1 to 550	Acetylene block applied to repacked cores	A horizon from agricultural soil	Soil water and C availability	*Weier et al.* [1993]
0 to 9	Acetylene block applied to soil suspensions	Agricultural soil	Redox potential	*Kralova et al.* [1992]
0.30 to 1.3	Acetylene block applied to moist sieved soil	Pasture soil upper 10 cm	NO_3^- and C	*Dendooven and Anderson* [1995]
0.68 to 7.1	Acetylene block applied to mixed and sieved soil	Forest grassland soils 20 cm	pH	*Sun et al.* [2012]
0.2 to 100	Direct N_2 measurement from intact cores	Mineral soil from spruce beech forests	Soil water and soil temperature	*Butterbach-Bahl et al.* [2002]
21 to 220	Direct N_2 measurement from intact cores	Forest floor and AH from a beech forest	Soil water, soil temperature, and pH	*Dannenmann et al.* [2008]
>130	Direct N_2 measurement from intact cores	Static chambers for N_2O; intact soil cores for N_2	Species and water table height	*Mander et al.* [2003]
5 to 55	Direct N_2 measurement from intact cores	Agriculture soil	NO_3^- and moisture	*Scheer et al.* [2009]
3 to 10	Direct N_2 measurement from intact cores	Agriculture soils	NO_3^-	*Wang et al.* [2013]

Precipitation events triggered N transformation processes that led to significantly more soil N_2O efflux from the OW topographic position. The observation that precipitation triggers soil N_2O efflux suggests that precipitation influences key physical and chemical properties that promote N_2O efflux. These responses include increasing soil moisture content, reducing O_2 concentration due to water occupying some of the soil pore spaces that result in low redox potential [*Li et al*., 1992; *Liptzin and Silver*, 2009; *Rubol et al*., 2012]. In the IW and OW, there was very little variation in soil moisture but much more variation in soil N_2O efflux (as indicated by the coefficients of dispersion), which suggests that precipitation may be the mechanism that controls soil N_2O flux. Precipitation events only triggered soil N_2O efflux episodes if the event exceeded the canopy interception capacity [*Carlyle-Moses and Price*, 1999; *Price and Carlyle-Moses*, 2003] and if the water table depth was less than 10 mm because at higher water table depths nutrients would bypass the bioactive layer and get flushed from the catchment into the stream [*Creed et al*., 1996]. Water table depths greater than 10 mm above the ground surface lead to inundated soils with slow diffusion of N_2O [*Arah*, 1997; *Teh et al*., 2011], which may have reduced the amount of N_2O efflux to the atmosphere, due to reduction to N_2 in the inundated soils.

Temperate forest soils contribute a substantial amount of N_2O and cannot be ignored in N budgets. Studies that have measured nitrification rates in upland versus wetland positions in sugar maple forests have demonstrated that the high soil moisture and consequent low redox potential result in very low rates of nitrification at wetland positions during the growing season [*Devito et al*., 1999; *Casson et al*., 2014]. Furthermore, nitrification is suppressed in soils with a pH lower than 4.5 [*Ste-Marie and Pare*, 1999], making nitrification an unlikely source of the observed N_2O. The NO_3^- observed at the OW position was likely flushed from the hillslope to the wetland during the rain event, not produced in situ via nitrification. Chemodenitrificaiton, another process which produces N_2O, is mainly observed in very acidic soils ($pH < 4$; *Kesik et al.* [2006]) and thus is likely to be a

minor mechanism at these study sites. The environmental conditions in the wetland make it very likely that the N_2O produced from these positions is a result of denitrification.

The increase in reactive atmospheric N and the inextricable link between precipitation, topography, soil redox potential, and soil N_2O efflux in temperate forests suggests that soil N_2O efflux will continue to be a substantial component of the N cycle. The finding that precipitation events trigger bursts of N_2O efflux emphasizes the interaction between long-term landscape determinants and short-term hydrological events in creating conditions appropriate for N_2O production. There is a need for more intensive monitoring of gaseous N fluxes and coupling hydrological models to these observations to produce robust, spatially explicit estimates of N_2O and N_2 effluxes in temperate forested catchments.

5. Conclusion

Denitrification is a key process of the forest N cycle, with N_2O and N_2 contributing to N transformations in the forest soils. While denitrification occurred at all topographic positions, it was more pronounced in wetland areas where appropriate redox conditions occur. Nitrous oxide and N_2 efflux from the wetland in response to effective precipitation events accounted for 16.1% of the annual N inputs. The wetland areas had greater potential for accumulation of denitrification precursors, mainly labile carbon (DOC) and NO_3^-, due to their relative position compared to the inclined upland areas in addition to the alternating redox potential between oxic and anoxic zones. The environmental determinants of denitrification in forest soils operate at different spatial and temporal scales making it challenging to derive catchment-specific estimates of gaseous N_2O and N_2 fluxes. Accurate estimates of these fluxes are needed both to quantify global warming effects associated with N_2O flux and to understand differences in the ways that forests process N across gradients of topography, climate, and N status.

Acknowledgments
This research was funded by an NSERC Discovery grant to IFC (217053-2009 RGPIN). Data are available by contacting Irena Creed (icreed@uwo.ca).

References

Addy, K. L., A. J. Gold, P. M. Groffman, and P. A. Jacinthe (1999), Ground water nitrate removal in subsoil of forested and mowed riparian buffer zones, *J. Environ. Qual.*, *28*, 962–970.

Ambus, P. (1998), Nitrous oxide production by denitrification and nitrification in temperate forest, grassland and agricultural soils, *Eur. J. Soil Sci.*, *49*, 495–502.

Ambus, P., and G. P. Roberston (2006), The effect of increased N deposition on nitrous oxide, methane and carbon dioxide fluxes from unmanaged forest and grassland communities in Michigan, *Biogeochemistry*, *79*, 315–337.

Anderson, T. R., P. M. Groffman, and M. T. Walter (2015), Using a soil topographic index to distribute denitrification fluxes across a northeastern headwater catchment, *J. Hydrol.*, *522*, 123–134.

Arah, J. R. M. (1997), Apportioning nitrous oxide fluxes between nitrification and denitrification using gas phase mass spectrometry, *Soil Biol. Biochem.*, *29*, 1295–1299.

Blanco-Jarvio, A., C. Chávez-López, M. Luna-Guido, L. Dendooven, and N. Cabirol (2011), Denitrification in a Chinampa soil of Mexico City as affected by methylparathion: A laboratory study, *Eur. J. Soil Biol.*, *47*, 271–278.

Butterbach-Bahl, K., G. Willibald, and H. Papen (2002), Soil core method for direct simultaneous determination of N_2 and N_2O emissions from forest soils, *Plant Soil*, *240*, 105–116.

Canada Soil Survey Committee (1978), *Canadian System of Soil Classification*, Department of Agriculture, Ottawa, Ontario, Canada.

Canada's National Forest Inventory (2013), Area of land cover by terrestrial ecozone in Canada. [Available at https://nfi.nfis.org/publications/standard_reports/pdf/NFI3_T1_LC_AREA_en.pdf, Accessed March 31, 2015.]

Carlyle-Moses, E., and A. G. Price (1999), An evaluation of the Gash interception model in a northern hardwood stand, *J. Hydrol.*, *214*, 103–110.

Casson, N. J., M. C. Eimers, and S. A. Watmough (2014), Controls on soil nitrification and stream nitrate export at two forested catchments, *Biogeochemistry*, *121*, 355–368.

Cirmo, C. P., and J. J. McDonnell (1997), Linking the hydrologic and biogeochemical controls of nitrogen transport in near-stream zones of temperate-forested catchments: A review, *J. Hydrol.*, *199*, 88–120.

Creed, I. F., L. E. Band, N. W. Foster, I. K. Morrison, J. A. Nicolson, R. S. Semkin, and D. S. Jeffries (1996), Regulation of nitrate-N release from temperate forest: A test of the N flushing hypothesis, *Water Resour. Res.*, *32*, 3337–3354.

Creed, I. F., J. F. Miller, D. A. Aldred, J. Adams, S. Spitale, and R. A. Bourbonniere (2013), Hydrologic profiling for greenhouse gas effluxes from natural grasslands in the prairie pothole region of Canada, *J. Geophys. Res. Biogeosci.*, *118*, 680–697, doi:10.1002/jgrg.20050.

Dannenmann, M., K. Butterbach-Bahl, R. Gasche, G. Willibald, and H. Papen (2008), Dinitrogen emissions and the N_2:N_2O emission ratio of a Rendzic Leptosol as influenced by pH and forest thinning, *Soil Biol. Biochem.*, *40*, 2317–2323.

Del Grosso, S. J., W. J. Parton, A. R. Mosier, D. S. Ojima, A. E. Kulmala, and S. Phongpan (2000), General model for N_2O and N_2 gas emissions from soils due to denitrification, *Global Biogeochem. Cycles*, *14*, 1045–1060.

Dendooven, L., and J. M. Anderson (1995), Maintenance of denitrification potential in pasture soil following anaerobic events, *Soil Biol. Biochem.*, *27*, 1251–1260.

Devito, K. J., C. J. Westbrook, and S. L. Schiff (1999), Nitrogen mineralization and nitrification in upland and peatland forest soils in two Canadian Shield catchments, *Can. J. For. Res.*, *29*, 1793–1804.

Dillon, P. J., L. A. Molot, and W. A. Schneider (1991), Phosphorus and nitrogen export from forested stream catchments in Central Ontario, *J. Environ. Qual.*, *20*, 857–864.

Duncan, J. M., P. M. Groffman, and L. E. Band (2013), Towards closing the watershed nitrogen budget: Spatial and temporal scaling of denitrification, *J. Geophys. Res. Biogeosci.*, *118*, 1105–1119, doi:10.1002/jgrg.20090.

Eshleman, K. N., R. D. Sabo, and K. M. Kline (2013), Surface water quality is improving due to declining atmospheric N deposition, *Environ. Sci. Technol.*, *47*(21), 12,193–12,200.
Foster, N., J. Spoelstra, P. Hazlett, S. Schiff, F. D. Beall, I. F. Creed, and C. David (2005), Heterogeneity in soil nitrogen within first-order forested catchments at the Turkey Lakes Watershed, *Can. J. For. Res.*, *35*, 797–805.
Gambrell, R. P., and W. H. Patrick Jr. (1978), Chemical and microbiological properties of anaerobic soils and sediments, in *Plant Life in Anaerobic Environments*, edited by D. D. Hook and R. M. Crawford, pp. 375–423, Ann Arbor Sci. Pub. Inc., Mich.
Groffman, P. M., M. A. Altabet, J. K. Bohlke, K. Butterbach-Bahl, M. B. David, M. K. Firestone, A. E. Giblin, T. M. Kana, L. P. Nielsen, and M. A. Voytek (2006), Methods for measuring denitrification: Diverse approaches to a difficult problem, *Ecol. Appl.*, *16*, 2091–2122.
Gu, J., B. Nicoullaud, P. Rochette, D. J. Pennock, C. Hénault, P. Cellier, and G. Richard (2011), Effect of topography on nitrous oxide emissions from winter wheat fields in Central France, *Environ. Pollut.*, *159*, 3149–3155.
Hall, M. K. D., A. J. Winters, and G. S. Rogers (2014), Variations in the diurnal flux of greenhouse gases from soil and optimizing the sampling protocol for closed static chambers, *Commun. Soil Sci. Plant Anal.*, *45*, 2970–2978.
Hazlett, P. W., and N. W. Foster (2002), Topographic controls of nitrogen, sulfur, and carbon transport from a tolerant hardwood hillslope, *Water Air Soil Pollut. Focus*, *2*, 63–80.
Hutchinson, G. L., and G. P. Livingston (2001), Vents and seals in non-steady-state chambers used for measuring gas exchange between soil and the atmosphere, *Eur. J. Soil Sci.*, *52*, 675–682.
Intergovernmental Panel on Climate Change (2013), *Climate Change 2013: The Physical Science Basis. Contribution of Working Group I to the Fifth Assessment Report of the Intergovernmental Panel on Climate Change*, edited by T. F. Stocker, Cambridge Univ. Press, Cambridge, U. K., and New York.
International Joint Commission (2012), Canada-United States air quality report 2012. [Available at https://www.ec.gc.ca/Publications/D9D6380B-4834-41C4-9D36-B6E3348F1A39/CanadaUnitedStatesAirQualityAgreementProgressReport2012.pdf.]
Jeffries, D. S., J. R. M. Kelso, and I. K. Morrison (1988), Physical, chemical, and biological characteristics of the Turkey Lakes Watershed, central Ontario, Canada, *Can. J. Fish. Aquat. Sci.*, *45*, 3–13.
Kesik, M., S. Blagodatsky, H. Papen, and K. Butterbach-Bahl (2006), Effect of pH, temperature and substrate on N_2O, NO and CO_2 production by *Alcaligenes faecalis* p, *J. Appl. Microbiol*, *101*, 655–667.
Kothawala, D. N., S. A. Watmough, M. N. Futter, L. Zhang, and P. J. Dillon (2011), Stream nitrate responds rapidly to decreasing nitrate deposition, *Ecosystems*, *14*(2), 274–286.
Kralova, M., P. H. Masscheleyn, C. W. Lindau, and W. H. Patarick Jr. (1992), Production of dinitrogen and nitrous oxide in soil suspensions as affected by redox potential, *Water Air Soil Pollut.*, *61*, 37–45.
Kulkarni, M. V., P. M. Groffman, J. B. Yavitt, and C. L. Goodale (2014), Complex controls of denitrification at ecosystem, landscape and regional scales in northern hardwood forests, *Ecol. Model.*, *298*, 39–52.
Li, C., S. Frolking, and T. A. Frolking (1992), A model of nitrous oxide evolution from soil driven by rainfall events: 1. Model structure and sensitivity, *J. Geophys. Res.*, *97*, 9759–9776.
Lindsay, J., and I. F. Creed (2006), Distinguising actual and artefact depressions in digital elevation data, *Comput. Geosci.*, *32*, 1192–1204.
Liptzin, D., and W. L. Silver (2009), Effects of carbon additions on iron reduction and phosphorus availability in a humid tropical forest soil, *Soil Biol. Biochem.*, *41*, 1696–1702.
Lohse, K. A., P. D. Brooks, J. C. McIntosh, T. Meixner, and T. E. Huxman (2009), Interactions between biogeochemistry and hydrologic systems, *Ann. Rev. Environ. Resour.*, *34*, 65–96.
Lovett, G. M., and C. L. Goodale (2011), A new conceptual model of nitrogen saturation based on experimental nitrogen addition to an oak forest, *Ecosystems*, *14*(4), 615–631.
Mander, U. E., V. Kuusemets, K. Lohmus, T. Mauring, S. Teiter, and J. Augustin (2003), Nitrous oxide, dinitrogen and methane emission in a subsurface flow constructed wetland, *Water Sci. Tech.*, *48*, 135–142.
McClain, M. E., et al. (2003), Biogeochemical hot spots and hot moments at the interface of terrestrial and aquatic ecosystems, *Ecosystems*, *6*, 301–312.
Menendez, S., R. J. Lopez-Bellido, J. Benıtez-Vega, C. Gonzalez-Murua, L. Lopez-Bellido, and J. M. Estavillo (2008), Long-term effect of tillage, crop rotation and N fertilization to wheat on gaseous emissions under rainfed Mediterranean conditions, *Eur. J. Agric.*, *28*, 559–569.
Mengistu, S. G., I. F. Creed, K. L. Webster, E. Enanga, and F. D. Beall (2014), Searching for similarity in topographic controls on carbon, nitrogen and phosphorus export from forested headwater catchments, *Hydrol. Process.*, *28*, 3201–3216.
Morse, J. L., J. Durán, F. Beall, E. M. Enanga, I. F. Creed, I. Fernandez, and P. M. Groffman (2015), Soil denitrification fluxes from three northeastern North American forests across a range of nitrogen deposition, *Oecologia*, *177*, 17–27.
Pardo, L. H., et al. (2011), Effects of nitrogen deposition and empirical nitrogen critical loads for ecoregions of the United States, *Ecol. Appl.*, *21*(8), 3049–3082.
Price, A. G., and D. E. Carlyle-Moses (2003), Measurement and modelling of growing-season canopy water fluxes in a mature mixed deciduous forest stand, southern Ontario, Canada, *Agric. For. Meteorol.*, *119*, 65–89.
Rubol, S., W. L. Silver, and A. Bellin (2012), Hydrologic control on redox and nitrogen dynamics in a peatland soil, *Sci. Total Environ.*, *432*, 37–46.
Scheer, C., R. Wassmann, K. Butterbach-Bahl, J. P. A. Lamers, and C. Martius (2009), The relationship between N_2O, NO, and N_2 fluxes from fertilized and irrigated dryland soils of the Aral Sea Basin, Uzbekistan, *Plant Soil*, *314*, 273–283.
Sirois, A., R. Vet, and D. MacTavish (2001), Atmospheric deposition to the Turkey Lakes Watershed: Temporal variations and characteristics, *Ecosystems*, *4*, 503–513.
Smith, W. B., P. D. Miles, C. H. Perry, and S. A. Pugh (2009), Forest resources of the United States, 2007 Gen. Tech. Rep. WO-78. Washington, D. C., U. S. Department of Agriculture, Forest Service, Washington Office.
Snider, D. M., S. L. Schiff, and J. Spoelstra (2009), $^{15}N/^{14}N$ and $^{18}O/^{16}O$ stable isotope ratios of nitrous oxide produced during denitrification in temperate forest soils, *Geochim. Cosmochim. Acta*, *73*, 877–888.
Speir, T. W., J. A. Townsend, R. D. More, and L. F. Hill (1999), Short-lived isotopic method to measure nitrous oxide emissions from a soil under four low-fertility management systems, *Soil Biol. Biochem.*, *31*, 1413–1421.
Ste-Marie, C., and D. Pare (1999), Soil, pH and N availability effects on net nitrification in the forest floors of a range of boreal forest stands, *Soil Biol. Biochem.*, *31*, 1579–1589.
Stewart, K. J., P. Grogan, D. S. Coxson, and S. D. Siciliano (2014), Topography as a key factor driving atmospheric nitrogen exchanges in arctic terrestrial ecosystems, *Soil Biol. Biochem.*, *70*, 96–112.
Sun, P., Y. Zhuge, J. Zhang, and Z. Cai (2012), Soil pH was the main controlling factor of the denitrification rates and N_2/N_2O emission ratios in forest and grassland soils along the Northeast China Transect (NECT), *Soil Sci. Plant Nutr.*, *58*, 517–525.
Teh, Y. A., W. L. Silver, O. Sonnentag, M. Detto, M. Kelly, and D. D. Baldocchi (2011), Large greenhouse gas emissions from a temperate peatland pasture, *Ecosystems*, *14*, 311–325.

Tiedje, J. M., S. Simkins, and P. M. Groffman (1989), Perspectives on measurement of denitrification in the field including recommended protocols for acetylene based methods, *Plant Soil*, *115*, 261–284.

Ullah, S., G. A. Breitenbeck, and S. P. Faulkner (2005), Denitrification and N_2O emission from forested and cultivated alluvial clay soil, *Biogeochemistry*, *73*, 499–513.

Vilain, G., J. Garnier, G. Tallec, and P. Cellier (2010), Effect of slope position and land use on nitrous oxide (N_2O) emissions (Seine Basin, France), *Agric. For. Meteorol.*, *150*, 1192–1202.

Wang, R., Q. Feng, T. Liao, X. Zheng, K. Butterbach-Bahl, W. Zhang, and C. Jin (2013), Effects of nitrate concentration on the denitrification potential of calcic cambisol and its fractions of N_2, N_2O and NO, *Plant Soil*, *363*, 175–189.

Webster, K. L., I. F. Creed, F. D. Beall, and R. A. Bourbonnière (2008a), Sensitivity of catchment-aggregated estimates of soil carbon dioxide efflux to topography under different climatic conditions, *J. Geophys. Res.*, *113*, G03040, doi:10.1029/2008JG000707.

Webster, K. L., I. F. Creed, R. A. Bourbonnière, and F. D. Beall (2008b), Controls on the heterogeneity of soil respiration in a tolerant hardwood forest, *J. Geophys. Res.*, *113*, G03018, doi:10.1029/2008JG000706.

Webster, K. L., I. F. Creed, F. D. Beall, and R. A. Bourbonnière (2011), A topographic template for estimating soil carbon pools in forested catchments, *Geoderma*, *160*, 457–467.

Weier, K. L., J. W. Doran, J. F. Power, and D. T. Walters (1993), Denitrification and the dinitrogen/nitrous oxide ratio as affected by soil water, available carbon, and nitrate, *Soil Sci. Soc. Am. J.*, *57*, 66–72.

Wickware, G. M., and D. W. Cowell (1985), Forest ecosystem classification of the Turkey Lakes Watershed, in *Environment Cons. Services*, *Lands Dir., Eco. Land. Class. Ser*, vol. 18, 33 pp., Can. Dep. Environ, Ontario.

Wrage, N., G. L. Velthof, M. L. van Beusichem, and O. Oenema (2001), Role of nitrifier denitrification in the production of nitrous oxide, *Soil Biol. Biochem.*, *33*, 1723–1732.

Yanai, R. D., M. A. Vadeboncoeur, S. P. Hamburg, M. A. Arthur, C. B. Fuss, P. M. Groffman, T. G. Siccama, and C. T. Driscoll (2013), From missing source to missing sink: Long-term changes in the nitrogen budget of a northern hardwood forest, *Environ. Sci. Technol.*, *47*, 11,440–11,448.

Yang, W. H., A. C. McDowell, P. D. Brooks, and W. L. Silver (2014), New high precision approach for measuring ^{15}N-N_2 gas fluxes from terrestrial ecosystems, *Soil Biol. Biochem.*, *69*, 234–241.

Zaman, M., and M. L. Nguyen (2010), Effect of lime or zeolite on N_2O and N_2 emissions from a pastoral soil treated with urine or nitrate-N fertilizer under field conditions, *Agric. Ecosyst. Environ.*, *136*, 254–261.

Zhu, Q., X. Nie, X. Zhou, K. Liao, and H. Li (2014), Soil moisture response to rainfall at different topographic positions along a mixed land-use hillslope, *Catena*, *119*, 61–70.